

## Development of a beta radioluminescence nuclear battery\*

XU Zhi-Heng (许志恒),<sup>1</sup> TANG Xiao-Bin (汤晓斌),<sup>1,†</sup>  
HONG Liang (洪亮),<sup>1</sup> LIU Yun-Peng (刘云鹏),<sup>1</sup> and CHEN Da (陈达)<sup>1</sup>

<sup>1</sup>Department of Nuclear Science and Engineering, Nanjing University of Aeronautics and Astronautics, Nanjing 211106, China

(Received December 18, 2013; accepted in revised form February 13, 2014; published online July 7, 2014)

A nuclear battery consisting of a beta source, a phosphor layer and a photovoltaic device was prepared. Planar phosphor layers were synthesized through physical precipitation of ZnS:Cu, ZnS:Ag or SrAl<sub>2</sub>O<sub>4</sub>:Eu<sup>2+</sup>, Dy<sup>3+</sup> phosphors. The radioluminescence (RL) spectra were used to analyze the RL effects of the phosphor layers under beta-particle excitation. Feasibility of using the materials as intermediate absorbers in the beta batteries was studied. The *I*-*V* characteristics of beta RL nuclear batteries with different phosphor layers were tested using <sup>63</sup>Ni or <sup>147</sup>Pm beta sources. The output power of zinc sulfide matrix phosphor layer was better than that of rare-earth element oxides. In addition, a thin aluminum reflective layer was vacuum-evaporated on the phosphor layers to improve the efficiency of beta RL nuclear batteries, and the results were discussed.

Keywords: Beta radioluminescence nuclear battery, Phosphor layer, Radioluminescence spectra, Current-voltage characteristic

DOI: 10.13538/j.1001-8042/nst.25.040603

### I. INTRODUCTION

Stable and efficient power systems with a long lifetime have tremendous potential applications in many fields, including ultra-low-power devices, autonomous systems, and aerospace electronics. In particular, the power sources can be used in places where their maintenance and replacement is extremely difficult or even impossible. Prime candidates for such power systems are radioisotope-motivated generators. A nuclear battery can convert nuclear power into usable electrical power for years, or even decades (depending on the radioactive isotope used). Other advantages of radioisotope power sources include small size, low weight, high adaptability, stable power output, and high reliability [1–6].

Performance of a beta-voltaic battery, based on ionization trails of high-energy electrons in a semiconductor, is limited by radiation damage to the semiconductor. An alternative to direct conversion of beta-voltaic batteries is to add a phosphor layer to absorb the beta-rays. The radiation energy is converted into luminescence energy, which is then converted into electricity [6, 7]. In this type of nuclear battery, a beta source is placed adjacent to the phosphor layer which absorbs energy of the beta particles and emits visible luminescence, which is immediately absorbed and converted into electricity by photovoltaic (PV) devices. The battery is advantageous in that the semiconductor itself no longer needs to be exposed directly to the ionizing radiations, hence the feasibility to minimize or eliminate radiation damage. Besides, the phosphor layers are more stable than PV devices [8]. So beta radioluminescence (RL) nuclear battery can adopt a radioisotope emitting

higher energy of beta particles. Even though the initial overall efficiency is lower, over a long term, the indirect power out is higher and the service life is longer than that of direct betavoltaics.

A schematic of the battery structure is shown in Fig. 1. Indirect energy conversion achieves two critical goals in nuclear batteries design: 1) high tolerance to ionizing radiations and high RL efficiency, and 2) appropriate matching of the emission wavelength to the spectral response of the PV device [9, 10]. Although the beta RL nuclear battery is still a long way from commercialization, research on this battery type is of significance. In this paper, we report the design, fabrication, and performance of beta RL nuclear batteries, which consist of (1) <sup>63</sup>Ni or <sup>147</sup>Pm beta emitter, (2) ZnS:Cu, ZnS:Ag or SrAl<sub>2</sub>O<sub>4</sub>:Eu<sup>2+</sup>, Dy<sup>3+</sup> phosphor layers, and (3) In-GaP/GaAs/Ge PV devices. The feasibility is examined for using different luminescent materials as phosphor layers of beta RL nuclear batteries, and batteries of different combinations are studied. In particular, performance of the batteries evaporated with an aluminum reflector on surface of the phosphor layer is presented.

### II. EXPERIMENTAL

#### A. Materials

In this work, we used thin circular plate beta source of <sup>63</sup>Ni and <sup>147</sup>Pm, in initial activity of 5 mCi/cm<sup>2</sup> on 11 August and 20 October, 2011, respectively. The <sup>63</sup>Ni and <sup>147</sup>Pm sources were selected with the following considerations. <sup>63</sup>Ni emits just 66.9 keV electrons, with a half-life of 100.2 y, while <sup>147</sup>Pm emits 224 keV electrons and weak low energy  $\gamma$ -ray, with a half-life of 2.6 y [11]. These provide better results comparison between them, easy shielding, and long-term use without significant performance degradation.

The RL phosphor layers were fabricated with ZnS:Cu, ZnS:Ag and SrAl<sub>2</sub>O<sub>4</sub>:Eu<sup>2+</sup>, Dy<sup>3+</sup>. These materials have been

\* Supported by the National Natural Science Foundation of China (No. 11205088), the Aeronautical Science Foundation of China (No. 2012ZB52021), the Fundamental Research Funds for the Central Universities, and the Foundation of Graduate Innovation Center in NUAA (No. kfjj130125)

† Corresponding author, tangxiaobin@nuaa.edu.cn

widely studied for field emission display and fluorescent lighting applications. They have been reported to function as RL phosphors under radioactive particle excitation [6, 7]. ZnS:Cu and ZnS:Ag are Cu<sup>2+</sup>- and Ag<sup>+</sup>-doped A<sub>2</sub>B<sub>6</sub>-based phosphor materials, respectively. ZnS-based phosphors have wide band gap and good conductivity. Their RL characteristics depends on the doping element, concentration and other factors [12]. The ratio of luminescence intensity between irradiated and non-irradiated ZnS:Cu phosphors is 0.95 by using 5.69 keV electrons. For ZnS:Ag phosphors, the ratio is 1 under the same beta source [7]. SrAl<sub>2</sub>O<sub>4</sub>:Eu<sup>2+</sup>, Dy<sup>3+</sup> phosphors are high-quality rare-earth-doped SrAl<sub>2</sub>O<sub>4</sub>-based material, with strontium aluminate as the matrix, and Eu<sup>2+</sup> and Dy<sup>3+</sup> as the activator systems [13]. The activator can change the band structure of the matrix and generate various RL energy levels. In the experiment, we used five kinds of phosphors: ZnS:Cu, ZnS:Ag and SrAl<sub>2</sub>O<sub>4</sub>:Eu<sup>2+</sup>, Dy<sup>3+</sup> of 200, 300 and 600 mesh, in particle sizes of 38 μm, 6.2 μm, 75 μm, 48 μm and 23 μm, respectively.

Given that different phosphor layers exhibit different luminescent performance, the emission wavelength range of the RL spectra is wide and inconsistent. Therefore, In-GaP/GaAs/Ge triple-junction PV devices are necessary to satisfy the wide range of RL emission spectra. The fabricated PV devices measured at 0.5 cm × 0.5 cm.

## B. Design and fabrication

A physical precipitation technique was performed to prepare different planar phosphor layers. The RL phosphors were deposited on quartz glass substrates in light transmittance of nearly 95%. The layer size was 3 cm × 3 cm (Fig. 2). For a planar geometry, the optimal phosphor layer must be of sufficient thickness to absorb most of beta particles and still allow for high-efficient transmission of the emitted luminescence. The relationship of the beta range and the phosphor layer thickness is the key to optimizing beta RL nuclear battery.

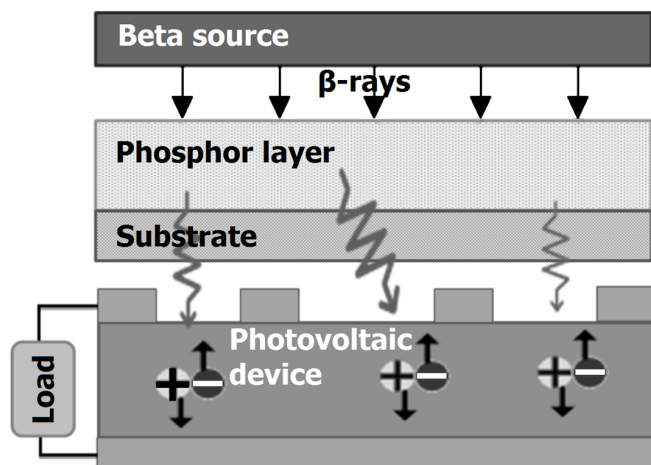


Fig. 1. Schematics of a beta RL nuclear battery.

The beta range of <sup>63</sup>Ni and <sup>147</sup>Pm was calculated with an empirical formula modified from Katz and Penfld [14]:

$$R = 0.412E^{1.265 - 0.0954 \ln E} / \rho, \quad E \leq 2.5 \text{ MeV}, \quad (1)$$

where  $R$  is the beta range in the phosphor layers (cm),  $E$  is the maximum energy of the beta source (MeV), and  $\rho$  is density of the phosphors (g/cm<sup>3</sup>). For <sup>63</sup>Ni,  $E = 66.9$  keV, and  $\rho = 4.102$  g/cm<sup>3</sup>, then  $R = 16.33$  μm.

Thickness of the phosphor layer was calculated by the following empirical formula:

$$d = \Delta m / (S\rho), \quad (2)$$

where,  $d$  is thickness of the phosphor layer,  $\Delta m$  is the weight difference between the starting and final glass,  $S$  is the surface area, and  $\rho$  is the density. Based on the preceding analysis, the thickness of ZnS:Cu phosphor layer was 27 μm, which was between the beta ranges of <sup>63</sup>Ni and <sup>147</sup>Pm in the ZnS:Cu phosphor layers.

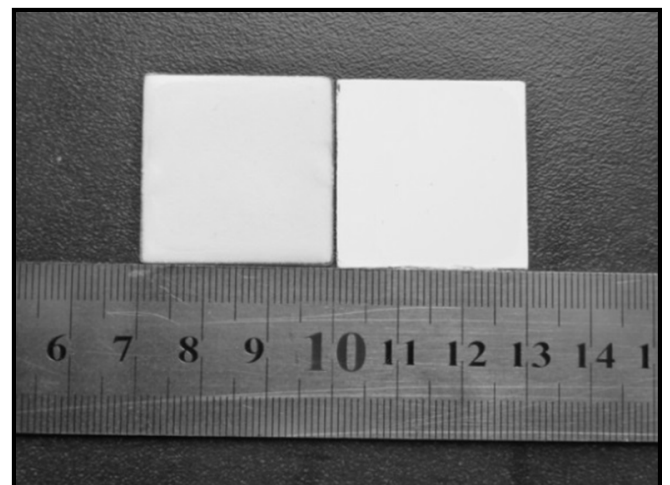


Fig. 2. Planar phosphor layer samples.

The phosphor layers, which functioned as intermediates, the beta source, and the PV devices were arranged and laminated according to Fig. 1. Design and fabrication were accomplished by arranging leads and encapsulating. The sequence of battery assembly is shown in Fig. 3. Fig. 3(d) shows the prototype of beta RL nuclear battery.

## C. Test method

RL spectra of the phosphor layers were measured by using a Cary Eclipse fluorescence spectrophotometer (Agilent Technologies, USA) with the 4.93 mCi/cm<sup>2</sup> <sup>63</sup>Ni and 2.83 mCi/cm<sup>2</sup> <sup>147</sup>Pm beta sources. To obtain an accurate and steady spectra, different phosphor layers were exposed to beta-particle irradiation for a distinct amount of time. Given that the afterglow time of rare-earth-doped strontium aluminate is relatively long, the SrAl<sub>2</sub>O<sub>4</sub>:Eu<sup>2+</sup>, Dy<sup>3+</sup> phosphor layers were observed for one hour or more. During the test period, the entire test environment was kept in a dark condition.

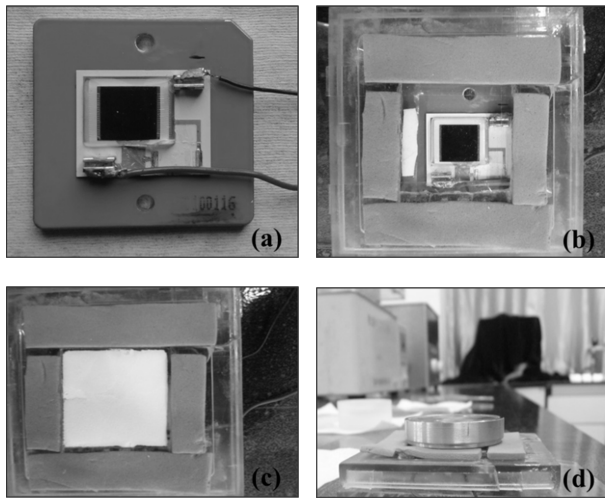


Fig. 3. Fabrication of beta RL nuclear battery: placing the PV device (a), and adding the support materials (b), phosphor layer (c), and beta source (d).

A dual-channel system (Model 2636A, Keithley, USA) was used to measure the current-voltage ( $I$ - $V$ ) and power-voltage ( $P$ - $V$ ) curves of various combinations with the  $^{63}\text{Ni}$  or  $^{147}\text{Pm}$  sources. Based on the test results, the following characteristics were determined: short-circuit current  $I_{sc}$ , open-circuit voltage  $U_{oc}$ , and maximum power output  $P_{max}$ . Moreover, external light interference should be avoided during the testing process to ensure that the phosphor layers would only be excited by the beta-particle source. All samples were tested at room temperatures and atmosphere.

### III. RESULTS AND DISCUSSION

#### A. Optical characterization

RL performances of the phosphor layers, namely, ZnS:Ag, ZnS:Cu, 200/300/600 mesh  $\text{SrAl}_2\text{O}_4:\text{Eu}^{2+}, \text{Dy}^{3+}$ , were measured under irradiation by  $4.93 \text{ mCi/cm}^2$   $^{63}\text{Ni}$  and  $2.83 \text{ mCi/cm}^2$   $^{147}\text{Pm}$  sources, respectively. The RL spectra were recorded after excitation RL became stable and were shown together in Fig. 4 for comparison.

The RL effect is obvious. A high RL yield reflects a high degree of crystallinity [15]. The phosphor layers exhibited different emission spectra for various luminescent materials. RL intensities of ZnS:Ag and ZnS:Cu are much higher than those of  $\text{SrAl}_2\text{O}_4:\text{Eu}^{2+}, \text{Dy}^{3+}$ . Comparing Fig. 4(a) with Fig. 4(b), the RL intensity of ZnS:Ag phosphor layers exhibited by  $^{63}\text{Ni}$  is much higher than the  $^{147}\text{Pm}$ -excited. This indicates that low-energy beta particles are suitable for ZnS:Ag phosphor layers of small particle sizes ( $6.2 \mu\text{m}$ ). ZnS:Ag and ZnS:Cu are high-efficiency yellow-green- and blue-emitting phosphors, at approximately 530 nm and 450 nm, respectively, under excitation by beta particles. This is mainly attributed to recombination of the electron trap donor from sul-

fur vacancy and the hole trap acceptor from the doped metal elements [12].

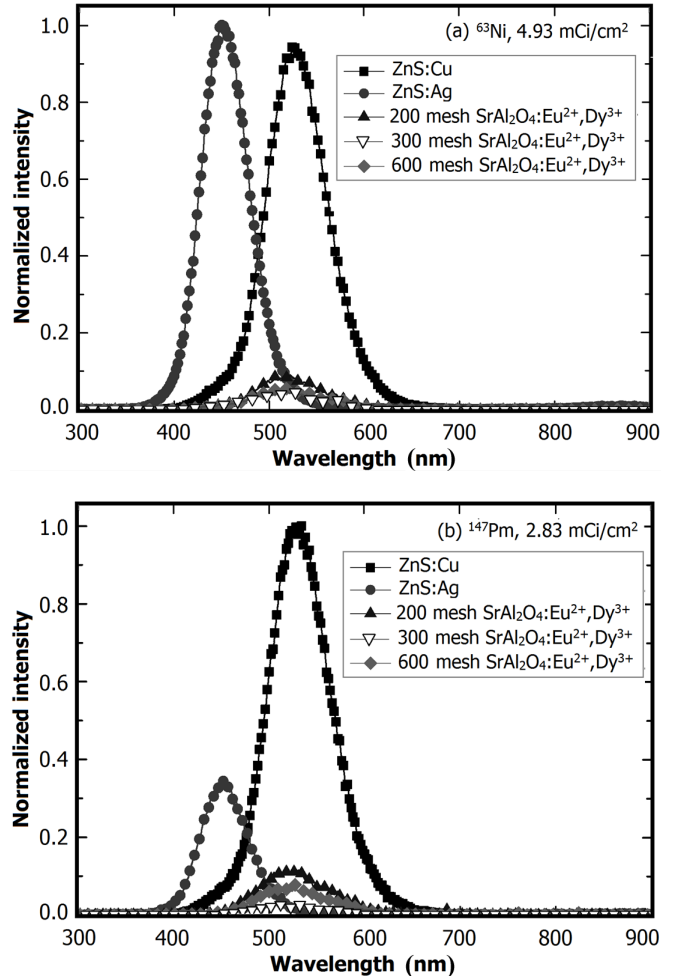


Fig. 4. RL spectra of different phosphor layers under excitation by (a)  $^{63}\text{Ni}$  and (b)  $^{147}\text{Pm}$  sources.

Comparing to ZnS:Cu and ZnS:Ag, RL intensity of the  $\text{SrAl}_2\text{O}_4:\text{Eu}^{2+}, \text{Dy}^{3+}$  phosphor layers is low under beta-particle excitation, peaked at approximately 520 nm, too. The peak attitude increases with particle size of the phosphors to a certain extent. These can be explained by two factors. First, phosphors of bigger particle size exhibit good crystallization and high RL efficiency. Second, a small particle size increases internal scattering and reduces emission intensity. Therefore, the luminescence transmission of big particle sizes is more significant and effective. This is consistent with results of Ref. [16], in which the scattering coefficient is calculated by the particle size distribution, with Eq. (3):

$$\ln s = \ln k - \ln g + 0.5 \ln^2 J, \quad (3)$$

where  $s$  is the scattering coefficient,  $k$  is a constant,  $g$  is the average particle size of the phosphors, and  $J$  is the standard deviation of the averaged particle size. According to this formula, as the average particle size  $g$  increases, the scattering coefficient  $s$  decreases.

Then, RL performance of the phosphors depends on the matrix material, doping element, and particle size.

### B. Electrical characterization

From the measured  $I$ - $V$  characteristic curves, we obtained the electronic performance parameters of the short-circuit current  $I_{sc}$ , the open-circuit voltage  $U_{oc}$ , and the maximum output power  $P_{max}$ . The fill factor FF can be calculated by Eq. (4):

$$FF = P_{max}/(I_{sc}U_{oc}). \quad (4)$$

The energy conversion efficiency of the beta RL nuclear battery is

$$\eta = P_{max}/(AE_{\beta}) = P_{max}/P_{source}, \quad (5)$$

where  $A$  is activity of the radioactive sources, and  $E_{\beta}$  is the average beta energy of 17.4 keV and 62 keV for  $^{63}\text{Ni}$  and  $^{147}\text{Pm}$ , respectively.

Figure 5 shows performances of the beta RL nuclear batteries of different phosphor layers. The ZnS:Cu phosphor layer exhibits efficient and stable performance. A nuclear battery with the  $^{63}\text{Ni}$  source, ZnS:Cu phosphor layer, and PV devices of InGaP/GaAs/Ge has with the following characteristics:  $I_{sc} = 1.0401 \text{ nA}$ ,  $U_{oc} = 0.3499 \text{ V}$ , and  $FF = 0.34$ . The activity of the source is

$$\begin{aligned} A_{source} &= 2^{-2.136/100.2} \times 5 \times 10^{-3} \times 3.7 \\ &\times 10^{10} \text{ s}^{-1} \text{ cm}^{-2} \times 0.25 \text{ cm}^2 \\ &= 4.5572 \times 10^7 \text{ s}^{-1}. \end{aligned} \quad (6)$$

The total output power of the source is

$$\begin{aligned} P_{source} &= 17.4 \times 10^{-3} \text{ MeV} \times 4.5572 \times 10^7 \text{ s}^{-1} \\ &\times 1.6022 \times 10^{-13} \text{ J/MeV} \\ &= 1.27 \times 10^{-7} \text{ W}. \end{aligned} \quad (7)$$

So, the energy conversion efficiency is

$$\eta = P_{max}/P_{source} = 9.81 \times 10^{-2}\%. \quad (8)$$

The performances of batteries with different phosphor layers are given in Table 1. The metal doped zinc sulfide phosphors exhibit better electrical characteristics than rare-earth-doped strontium aluminate. The RL emission wavelengths of ZnS:Ag phosphor layers are relatively short, and of high luminescence energy. However, the energy conversion efficiency of ZnS:Ag phosphor layers is significantly lower than that of ZnS:Cu phosphor layers. The peak emission of the phosphor layers matches peak response of the PV converter, and output performance of the battery is good. The luminescent energy ( $E_{\lambda}$ , in eV) can be related with the RL wavelength ( $\lambda$ , in nm) by:

$$E_{\lambda} = 1240/\lambda. \quad (9)$$

The luminescent energy of ZnS:Cu phosphor layers ( $\sim 2.34$  eV) is lower than that of ZnS:Ag ( $\sim 2.76$  eV). However, the ZnS:Cu phosphor layers have closer band gap to those of InGaP/GaAs/Ge PV devices (band gap = 1.90/1.46/0.7 eV). The electrical characteristics improve with higher degree of coupling. For example, the peak emission of  $\text{SrAl}_2\text{O}_4:\text{Eu}^{2+}, \text{Dy}^{3+}$  at 520 nm, is suitable for conversion by InGaP/GaAs/Ge PV devices. Nevertheless, luminescence intensity of the  $\text{SrAl}_2\text{O}_4:\text{Eu}^{2+}, \text{Dy}^{3+}$  was extremely low, and the luminescence received by the PV converter was minimal, such that the output power of the battery was nearly zero.

Also, the results illustrate that the RL emission wavelength and RL intensity of phosphor layers are important factors that affect performance of the beta RL nuclear battery. The RL from the phosphor layers is a critical step towards realizing the indirect energy conversion. The peak emission and band gap of the PV materials have a corresponding relation. By analyzing the RL spectra, appropriate band-gap range of the subsequent PV materials can be estimated. For

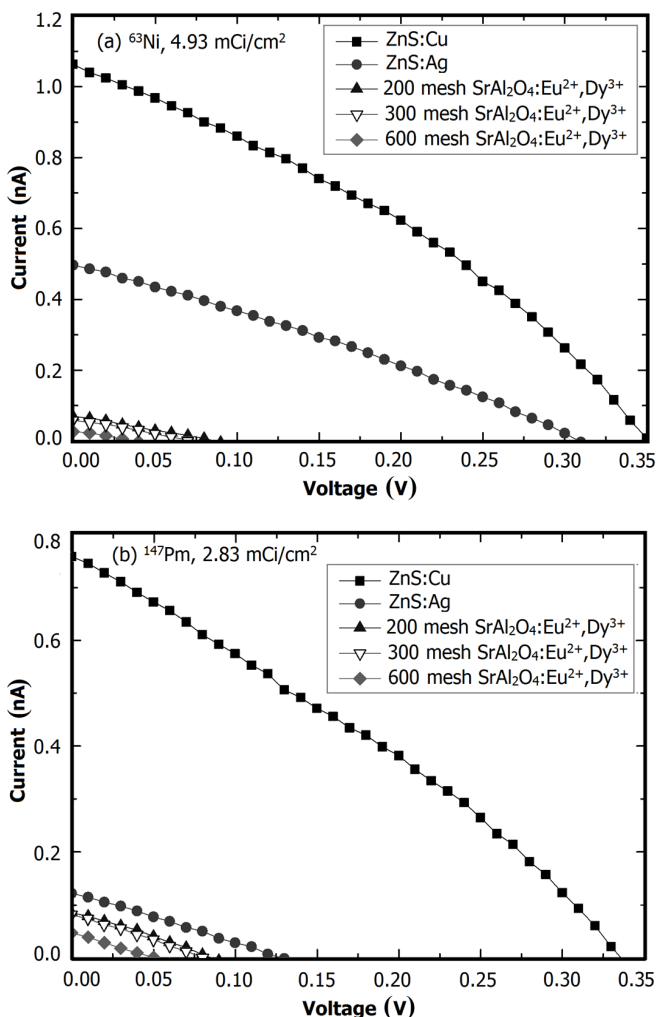


Fig. 5.  $I$ - $V$  characteristic curves of the batteries of different phosphor layers using (a)  $^{63}\text{Ni}$  and (b)  $^{147}\text{Pm}$  sources.

TABLE 1. Test data of the battery with different phosphor layers

Measured objects	$I_{sc}$ (nA)		$U_{oc}$ (V)		$FF$		$P_{max}$ (nW)		$\eta$ (%)	
	$^{63}\text{Ni}$	$^{147}\text{Pm}$								
ZnS:Cu	1.0401	0.7442	0.3499	0.3299	0.34	0.31	0.1246	0.0763	0.0981	0.0294
ZnS:Ag	0.4858	0.1145	0.2999	0.1199	0.31	0.29	0.0453	0.0040	0.0356	0.0016
200 mesh	0.0645	0.0791	0.0799	0.0799	0.30	0.33	0.0015	0.0021	0.0012	0.0008
300 mesh	0.0527	0.0740	0.0699	0.0799	0.33	0.30	0.0012	0.0018	0.0009	0.0007
600 mesh	0.0227	0.0396	0.0299	0.0499	0.45	0.29	0.0003	0.0006	0.0002	0.0002

beta RL nuclear battery, appropriate coupling among the radiation source, the phosphor layers and PV devices are required to achieve maximum nuclear-to-electrical energy conversion efficiency.

### C. Technology improvement

To improve performance of the beta RL nuclear battery, one should increase the RL efficiency and optimize the optical transmission properties. This involves depositing a thin reflective metal layer onto surface of the phosphor layers. Reducing the loss of photons, and increasing the luminescent intensity effectively, are helpful. Of all the phosphor layers tested, ZnS:Cu is the most stable and efficient. Aluminum reflector of 1  $\mu\text{m}$  thick was deposited on the ZnS:Cu phosphors by vacuum evaporation, and the batteries were excited by the  $^{63}\text{Ni}$  or  $^{147}\text{Pm}$  beta source. Performance of the beta RL nuclear batteries before and after aluminizing is shown in Fig. 6 and Table 2.

From the  $I$ - $V$  and  $P$ - $V$  characteristic curves, the maximum output power of the battery with a promethium source increased after aluminizing. However, for the nickel source, the energy conversion efficiency decreased obviously after aluminizing. The performance of the phosphor layers before and after aluminizing was affected by beta particle absorption and photon utilization.

Given that light emission is isotropic in the phosphor layers, the intensity of light emitted toward the source is the same as that emitted toward the PV device. The aluminum reflector increases the reflected luminescence from the phosphor layer towards the source, hence the increase of luminescent flux on the PV device. However, the aluminum reflector obstructs beta particles in the phosphor layers, hence the decrease of photon number and RL intensity. The foil also adds a certain thickness, extends photonic transport distance, and decreases the total output performance of the battery.  $^{147}\text{Pm}$  emits the beta particles of higher energies than  $^{63}\text{Ni}$  does, hence their longer ranges in the phosphor, of which the photon reflection increase effect can be stronger than its electron blocking and absorption effects. Therefore, performance of  $^{147}\text{Pm}$ -excited beta RL nuclear battery with an aluminum reflector is improved, with a gain of about 14% in energy conversion efficiency. For an alpha RL nuclear battery with a  $^{238}\text{Pu}$  source, the efficiency could be improved obviously by adding an aluminum reflector, with an increase of about 60% in the power output [8]. Unlike the  $^{147}\text{Pm}$  battery, aluminizing on the phosphor layer of  $^{63}\text{Ni}$ -excited nuclear battery re-

sults in its performance degradation. Therefore, the beta-ray energy should be considered to decide the necessity of aluminizing on the surface of the phosphor layers in preparing of the beta RL nuclear battery.

### IV. CONCLUSION

Three types of phosphor layers for beta RL nuclear battery were investigated via the RL spectra. From the  $I$ - $V$

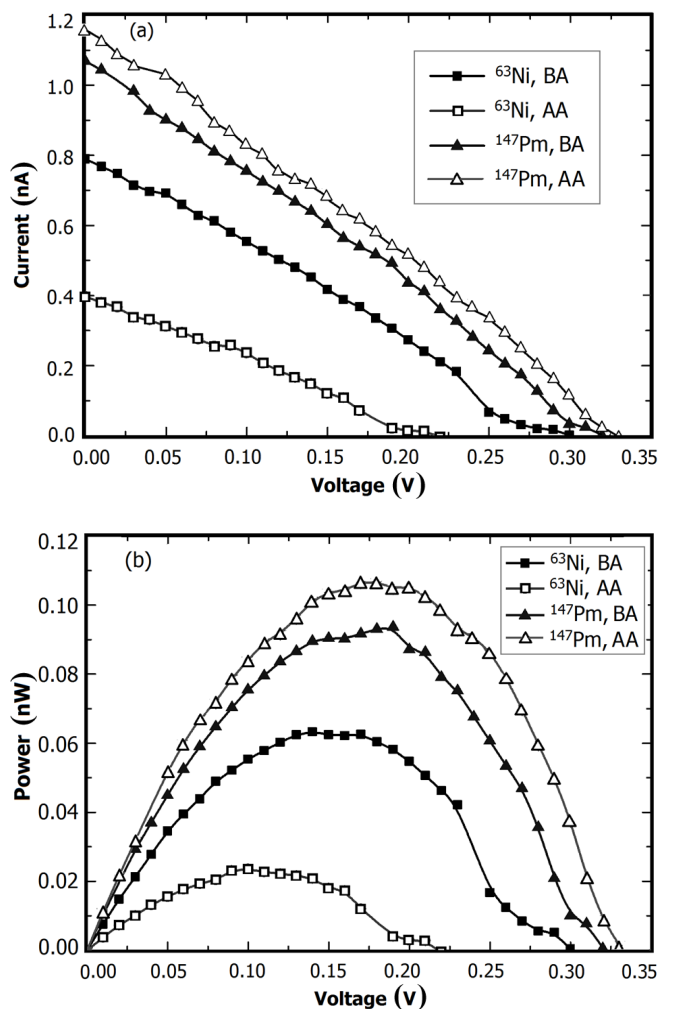


Fig. 6.  $I$ - $V$  (a) and  $P$ - $V$  (b) curves of the batteries of ZnS:Cu before and after aluminizing (referred as BA and AA).

TABLE 2. Test data of the phosphor layers before and after aluminizing (referred as BA and AA)

Samples	$I_{sc}$ (nA)		$U_{oc}$ (V)		$FF$		$P_{max}$ (nW)		$\eta$ (%)	
	$^{63}\text{Ni}$	$^{147}\text{Pm}$								
BA	0.7898	1.0693	0.2999	0.3199	0.2641	0.2738	0.0625	0.0936	0.0492	0.0329
AA	0.3979	1.1614	0.2198	0.3299	0.1538	0.2783	0.0236	0.1066	0.0186	0.0374

characteristic curves, output performance of the batteries was largely determined by RL wavelength and intensity. Comparing the results from different combinations of beta sources and phosphor layers, the RL performance of metal-doped zinc sulfide was better than that of rare-earth-doped strontium aluminate, and ZnS:Cu phosphor layers were more suitable than

ZnS:Ag to coupling with the InGaP/GaAs/Ge PV devices of the beta RL nuclear battery. Efficiency of the beta RL nuclear battery was determined by the beta particle reflection, the thickness of the phosphor layers, the RL transmission efficiency, and the coupling degree of the RL spectra and the PV devices. Some of the factors were studied.

[1] Qiao D Y, Chen X J, Ren Y, *et al.* *Acta Phys Sin-Ch Ed*, 2011, **60**: 020701.

[2] Tang X B, Liu Y P, Ding D, *et al.* *Sci China Tech Sci*, 2012, **55**: 659–664.

[3] Gao H, Luo S Z, Zhang H M, *et al.* *Acta Phys Sin-Ch Ed*, 2012, **61**: 176101.

[4] Peng Z X, Zhang P, He Z H. *Nucl Tech*, 2010, **33**: 308–311.

[5] Rivenburg H C, Bilhuber P, Divers III E F, *et al.* US Patent 5 443 657, Power source using a photovoltaic array and self-luminous microspheres, 1995.

[6] Sims P E, Dinetta L C, Barnett A M. 13<sup>th</sup> Space Photovoltaic Research and Technology Conference Cleveland, Ohio, Jun.14–16, 1994.

[7] Bower K E, Barbanel Y A, Shreter Y G, *et al.* Polymers, phosphors, and voltaics for radioisotope microbatteries. Boca Raton (USA): CRC Press, 2002, 210–348.

[8] Sychov M, Kavetsky A, Yakubova G, *et al.* *Appl Radiat Isotopes*, 2008, **66**: 173–177.

[9] Renschler C L, Clough R L, Sheppard T J. *J Appl Phys*, 1989, **66**: 4542–4544.

[10] Cress C D, Redino C S, Landi B J, *et al.* *J Solid State Chem*, 2008, **181**: 2041–2045.

[11] Sun S Z. *Radioisotope handbook*. Beijing (CHINA): Atomic Energy Press, 2011, 53–76.

[12] Cress C D. Ph.D. Thesis, Rochester Institute of Technology, 2008.

[13] Xiao Z G and Luo X X. *Light-Storing Material and Products*. Beijing (CHINA): Chemical industry press, 2002, 74–81.

[14] Liu Q C, Jia B S, Wan J. *Overview of Nuclear Science*. Harbin (CHINA): Harbin Institute of Technology Press, 1988, 32–33.

[15] Yen W M and Yamamoto H. *Phosphor handbook*. Boca Raton (USA): CRC Press, 2012, 388–618.

[16] Butler K H. *Fluorescent Lamp Phosphors: Theory and Technology*. Pennsylvania State (USA): Pennsylvania State University Press, 1980, 132–168.